Comparative FTIR Analysis of the Microenvironment of $Q_A^{-\bullet}$ in Cyanide-Treated, High pH-Treated and Iron-Depleted Photosystem II Membrane Fragments†

T. Noguchi,‡ J. Kurreck,§ Y. Inoue,‡ and G. Renger*,§

Photosynthesis Research Laboratory, The Institute of Physical and Chemical Research (RIKEN), Wako, Saitama 351 0198, Japan, and Max Volmer Institute for Biophysical Chemistry and Biochemistry, Technical University Berlin, Strasse des 17. Juni 135, 10623 Berlin, Germany

Received July 21, 1998; Revised Manuscript Received January 13, 1999

ABSTRACT: FTIR difference spectra due to light-induced $Q_A^{-\bullet}$ formation were measured in control PS II membrane fragments and in samples where the magnetic interaction with the non-heme iron center in its high-spin Fe^{2+} state is eliminated by three different methods, i.e., extraction of the non-heme iron center, treatment with cyanide, and incubation at high pH (pH = 11). The results obtained reveal that (i) the most pronounced band at 1479 cm^{-1} reflecting the C⋯O stretching mode of $Q_A^{-\bullet}$ in the semiquinone anion radical remains invariant to "iron depletion" while it shifts by 4 and 2 cm^{-1} to lower frequencies upon cyanide and high pH treatments, respectively, (ii) peaks observed in the 2600−3000 cm^{-1} region which arise from Fermi resonance of harmonics and combinations of the imidazole ring modes with the hydrogen-bonding NH stretching vibrations are not affected upon iron depletion but are lost in cyanide and high pH-treated samples, and (iii) all three treatments give rise to some similar changes in the amide I bands of the protein backbones and in imidazole ring modes of the coupled histidine. These results show that the hydrogen-bonding interaction of $Q_A^{-\bullet}$ is virtually unaffected upon non-heme iron depletion; in particular, the strong hydrogen bond between Q_A and a histidine side chain (most likely His 215 of the D2 subunit) is not changed. In marked contrast, drastic changes take place in the hydrogen bonding between Q_A and His upon CN^- and high pH treatments. The straightforward interpretation is that the hydrogen bond is lost upon these treatments. Despite the striking difference in the effect of hydrogen-bonding interaction, all three treatments lead to similar structural pertubations on the protein conformational changes due to $Q_A^{-\bullet}$ formation and ring vibrations of the coupled histidine side chain. On the basis of the data presented in the study, it is inferred that, concerning the hydrogen bond interaction, the microenvironment of $Q_A^{-\bullet}$ is close to the native state when a suitable iron depletion is performed. Accordingly, the previously reported conclusion on the hydrogen-bonding pattern of $Q_A^{-\bullet}$ in PS II [MacMillan, F., Lendzian, F., Renger, G., and Lubitz, W. (1995) *Biochemistry 34*, 8144−8156] studied by using iron-depleted preparations most likely reflects the situation in an intact PS II.

The essential steps of photosynthetic water cleavage take place in a multimeric protein complex, photosystem II (PS II),[1] which is anisotropically incorporated into the thylakoid membrane. The overall reaction in PS II leads to formation of molecular oxygen which is released into the atmosphere and bound hydrogen in the form of plastoquinol (PQH_2) (for a recent review, see ref *1*). The latter process occurs via a sequence of two single electron transfer steps at a plastoquinone (PQ) molecule transiently bound to a special protein pocket referred to as the Q_B site. This process is driven by the semiquinone anion radical $Q_A^{-\bullet}$ acting as reductant (for reviews, see refs *2* and *3*). The functional and structural organization of PQH_2 formation in PS II closely resembles that of UQH_2 in anoxygenic purple bacteria (*2*−*5*). Likewise, in both cases, the electron transfer from $Q_A^{-\bullet}$ to Q_B appears to be coupled with marked dynamic structural changes of Q_B (*6*−*8*). Another characteristic feature is the presence of a high-spin non-heme iron which is located between Q_A and Q_B. In purple bacterial reaction centers (RC) this Fe^{2+} is known to be coordinated by four histidine residues (two from each of the L and M subunits of the heterodimer forming the RC apoprotein) and one glutamate (*9*, *10*). An analogous ligation of Fe^{2+} by four histidines from polypeptides D1 and D2 is assumed to exist in PS II (*4*, *5*) while the glutamate is replaced by bicarbonate as a bidentate ligand (*11*). The latter change is probably a major factor

† This work was supported by the Eminent Scientist Program of RIKEN (to G.R.), by the Deutsche Forschungsgemeinschaft (G.R. and J.K.), and by grants for Photosynthetic Sciences and the Biodesign Research Program at RIKEN given by the Science and Technology Agency (STA) of Japan (T.N. and Y.I.).

* Corresponding author.
‡ The Institute of Physical and Chemical Research.
§ Technical University Berlin.

[1] Abbreviations: Chl, chlorophyll; CW, continuous wave; DCMU, 3-(3,4-dichlorophenyl)-1,1-dimethylurea; ENDOR, electron nuclear double resonance; EPR, electron paramagnetic resonance; ESEEM, electron spin-echo envelope modulation; FTIR, Fourier transform infrared; PS II, photosystem II; P680, primary donor of PS II; Q_A and Q_B, primary and secondary quinone acceptors in PS II; PQ, plastoquinone; PQH_2, plastoquinol; RC, reaction center; UQH_2, ubiquinol; WOC, water-oxidizing complex; Y_Z and Y_D, tyrosine 161 of the D1 and D2 proteins, respectively.

10.1021/bi981759e CCC: $18.00
Published on Web 03/23/1999

which is mainly responsible for the marked shift of the redox potential of the non-heme iron toward lower values in PS II (*12*−*14*).

The functional role of this iron center is not yet clarified, but regardless of this unresolved problem, it is very important for the application of different spectroscopic techniques as analytical tools for studies of PS II. Two opposite effects arise: (i) the "replacement" by ^{57}Fe offers the possibility of applying Mössbauer spectroscopy to analyze the coordination sphere of the non-heme iron center (*15*) and the protein dynamics and studying its correlation with electron transfer from $Q_A^{-\bullet}$ to Q_B in both purple bacteria (*16*) and PS II (*8*, *17*); (ii) on the other hand, the magnetic moment of the high-spin Fe^{2+} leads to strong magnetic coupling with other radical species and thereby hampers the application of sensitive magnetic resonance methods. In principle, three basically different methods can be used to circumvent the latter problem: (i) transfer of the high-spin to the low-spin $S = 0$ form by treatment with high concentrations of cyanide (*18*, *19*) or high pH (pH 11) (*20*), (ii) replacement of Fe^{2+} by diamagnetic cations like Zn^{2+} (*21*, *22*), or (iii) removal of the non-heme iron center (*23*, *24*). The latter goal was achieved by the development of a specific method which permits the extraction of the non-heme iron below the detection limit of Mössbauer spectroscopy (*24*). The heme iron is not extracted. Therefore, this sample type is referred to as "iron depleted" to indicate that they are lacking only the non-heme iron.

Using the "iron depletion" method, pulsed EPR spectroscopic studies could be performed to unravel the distances from $Q_A^{-\bullet}$ to $P680^{+\bullet}$ and $Q_A^{-\bullet}$ to Y_Z^{OX}. A precise value of 27 ± 0.3 Å was determined for the distance between $Q_A^{-\bullet}$ and $P680^{+\bullet}$ whereas only an estimation of 35 ± 3 Å could be achieved for the radical pair $Q_A^{-\bullet}$ Y_Z^{OX} (*25*). A more precise value for the latter distance (34 ± 1 Å) was recently obtained for pH = 11 treated samples due to markedly accelerated electron transfer from Y_Z to $P680^{+\bullet}$ (*26*). ENDOR and ESEEM spectroscopies were applied to probe the microenvironment of $Q_A^{-\bullet}$. It was found that in iron-depleted PS II membrane fragments the hydrogen bonding of $Q_A^{-\bullet}$ is somewhat altered compared with that of $PQ\text{-}9^{-\bullet}$ in frozen solution but similar to that of $Q_A^{-\bullet}$ in reaction centers from purple bacteria (*27*). Likewise, the interaction with nitrogen from the peptide backbone and possibly also with the N^{δ}−H of a histidine residue exhibits striking similarities in PS II and purple bacteria (*28*). However, the above mentioned data might not reflect the in situ interactions of the intact system because the removal of the non-heme iron center is expected to change its microenvironment. This might also affect the neighborhood of $Q_A^{-\bullet}$. A comparative analysis of the functional pattern revealed that the kinetics of Q_A formation by electron transfer from $Pheo^{-\bullet}$ remain almost unaffected in iron-depleted PS II membrane fragments whereas a marked retardation is observed in CN^--treated samples (*28*). This finding suggests that the iron-depleted preparation is superior for analyzing the environment of $Q_A^{-\bullet}$, but it does not provide direct information on the extent of deviation from a native PS II. Therefore, it is highly desirable to use complementary methods which are sensitive to structural modifications near $Q_A^{-\bullet}$ and simultaneously permit comparative studies between untreated and iron-depleted PS II membrane fragments. FTIR difference spectroscopy provides the most promising tool to achieve this goal. The present study provides results obtained in iron-depleted and CN^--treated samples and of PS II membrane fragments where the magnetic interaction of $Q_A^{-\bullet}$ with high-spin Fe^{2+} is eliminated by pH = 11 treatment (*20*). They show that the hydrogen bonding of $Q_A^{-\bullet}$ remains virtually unaffected by removal of the non-heme iron, whereas more severe changes arise due to pH = 11 and especially CN^- treatment.

MATERIALS AND METHODS

PS II membrane fragments from spinach were prepared according to the method of Berthold et al. (*29*) with slight modifications as described in ref 30. Iron depletion was performed by a method that is described in refs *23* and *27*. The iron depletion procedure was improved by incubating the PS II membrane fragments twice with $LiClO_4$, 1,10-phenanthroline, and conalbumin as outlined in ref *24*. After the final isolation step the material was suspended in 10 mM MES−NaOH (pH = 6.5), 15 mM NaCl, 4 mM $MgCl_2$, and 0.4 M sucrose. These samples were frozen in small aliquots in liquid nitrogen and stored at −80 °C until used.

After thawing, 60 μL of the control (8.3 mg of Chl/mL) or 100 μL of iron-depleted PS II membrane fragments (5 mg Chl/mL) was washed once with a buffer solution containing 20 mM NaCl, 400 mM sucrose, and either 40 mM MES−NaOH (pH = 6.5) or 40 mM Tris-HCl (pH = 8.5), centrifuged, and resuspended in 1 mL of the same buffer. For the cyanide treatment, the Mn cluster was removed by incubating the membranes (0.5 mg of Chl/mL) in 0.8 M Tris-HCl (pH 8.5) for 1 h on ice under room light followed by resuspension in a buffer containing 60 mM Hepes−NaOH (pH 8.0), 400 mM sucrose, and 10 mM NaCl. The Tris-treated membranes were then incubated with 350 mM KCN at pH 8.0 for 3 h on ice. The high pH treatment was done by resuspending the Tris-treated PS II membranes in a buffer containing 50 mM glycine−NaOH (pH 11), 400 mM sucrose, 10 mM NaCl, and 1 mM NaEDTA. Following addition of NH_2OH (10 mM) and DCMU (0.1 mM), the above PS II suspensions were centrifuged for 40 min at 170000*g*. The pellet obtained was finally sandwiched between a pair of BaF_2 plates.

FTIR spectra were measured with a JEOL JIR-6500 spectrophotometer equipped with a MCT detector (EG & G Judson IR-DET 101) as described previously (*31*, *32*). The sample temperature was adjusted to 250 K in a liquid N_2 cryostat (Oxford DN 1704) using a controller (Oxford ITC 4). Difference spectra were obtained by subtraction between the two single beam spectra (150 s accumulation for each) measured before and after illumination with red CW light (>600 nm) for 5 s. Two spectra measured with different samples were averaged for each final spectrum.

RESULTS AND DISCUSSION

Iron-Depleted Samples. In order to obtain an FTIR difference spectrum of $Q_A^{-\bullet}$ which is not "contaminated" by other redox-active species, e.g., Y_Z^{OX}/Y_Z or Y_D^{OX}/Y_D, the samples were preincubated with DCMU (100 μM) and NH_2-OH (10 mM). The former substance prevents $Q_A^{-\bullet}$ reoxidation by Q_B ($Q_B^{-\bullet}$), and the latter one destroys the water-

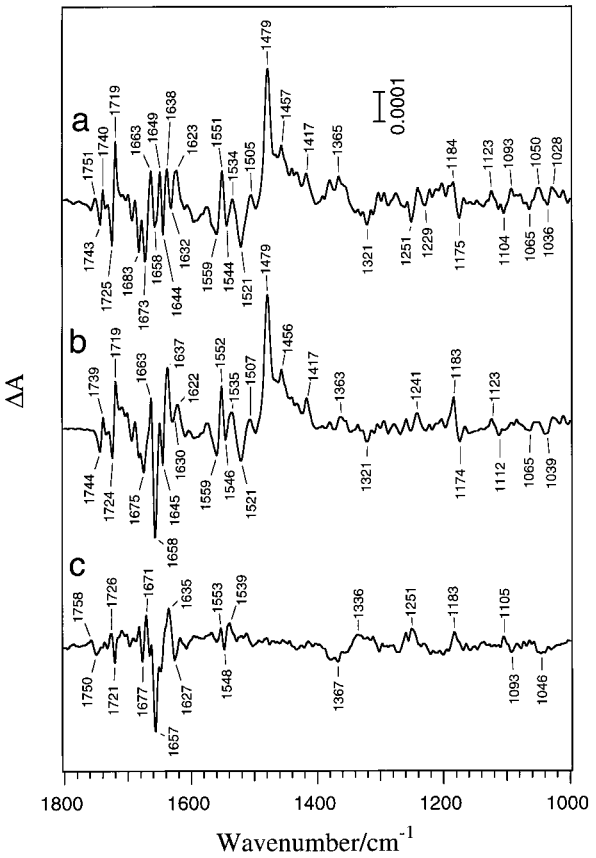

FIGURE 1: Light-induced FTIR difference spectra of PS II upon $Q_A^{-\bullet}$ formation measured in PS II membrane fragments from spinach (trace a) and samples deprived from the non-heme iron center (trace b). Trace c is the difference of the difference spectra a and b (spectrum b minus spectrum a). For experimental details, see Materials and Methods.

oxidizing complex (WOC) of the control sample (iron-depleted samples are already completely deprived of oxygen evolution capacity; see ref 28) and simutaneously acts as an electron donor, thus suppressing contributions due to light-induced oxidation of tyrosines Y_Z and Y_D. This procedure assures that $Q_A^{-\bullet}$ remains reduced for a long time.

The light-induced FTIR difference spectrum obtained in the control samples at pH = 6.5 is shown as the top trace (a) of Figure 1. An inspection of these data readily shows that a band pattern emerges which is characteristic for the difference spectrum of $Q_A^{-\bullet}/Q_A$ in PS II (*33*, *34*), the most prominent positive peak at 1479 cm^{-1} reflecting the C⋯O stretching mode of $Q_A^{-\bullet}$ and the negative bands at 1644 and 1632 cm^{-1} which are possible candidates for the C═O stretching modes of neutral Q_A. The 1725/19 cm^{-1} bands in the range of protonated carboxylic group(s) (Asp, Glu residues) and of the C_{10}═O ester bond of pheophytin and the characteristic changes at 1683 and 1673 cm^{-1} in the amide I region and at 1559/1551/1544 cm^{-1} in the amide II region are assigned as outlined in refs *33* and *34*. The corresponding light-induced difference spectrum of iron-depleted PS II membrane fragments is shown in the middle trace (b) of Figure 1. At first glance it is readily seen that, with respect to the typical $Q_A^{-\bullet}/Q_A$ bands, the spectrum exhibits striking similarities to that of the control containing the non-heme iron whereas in the region of the amide I band differences between both samples emerge. In order to permit a closer inspection, the difference of the difference spectra a and b (spectrum b minus spectrum a) was calculated and depicted at the bottom (trace c) of Figure 1. The following features emerge from these data: (i) Changes of the C⋯O stretching mode of $Q_A^{-\bullet}$ caused by the removal of the non-heme iron are below the detection limit of the measurements. (ii) Some changes arise in the amide I region of the protein backbone vibrations: a positive peak at 1637 cm^{-1} and a negative peak at 1658 cm^{-1} become more pronounced, and a negative peak at 1683 cm^{-1} becomes less pronounced. (iii) Several peaks are detectable in the lower frequency region at 1367/1336, 1251, 1183, 1105/1093, and 1046 cm^{-1} in the double difference spectrum.

The first result is of high relevance because it indicates that the hydrogen bonding of the semiquinone $Q_A^{-\bullet}$ (see ref *27* and references therein) remains virtually unaffected by removal of the non-heme iron center. As a consequence, the previously reported highly asymmetric hydrogen bonding of $Q_A^{-\bullet}$ in iron-depleted samples (*27*) most likely reflects the pattern of native PS II containing the non-heme iron.

The changes in the amide I region indicate some perturbation of the protein conformation and/or its rearrangement upon $Q_A^{-\bullet}$ formation in iron-depleted samples. When considering possible changes in the structural response owing to $Q_A^{-\bullet}$ formation in iron-depleted PS II membrane fragments, it appears worth taking into account modeling studies on the geometry of the environment of the Fe^{2+} and Q_A. On the basis of recent proposals (*35*, *36*) removal of the non-heme iron center is expected to cause a loss of bicarbonate and rearrangement of histidines 215 and 272 of polypeptide D1 and histidines 215 and 269 of polypeptide D2 (for numbering of residues for higher plants, see ref *35*). Accordingly, bands assigned to histidine vibrations are of special interest. Recently, histidine bands were identified in the $Q_A^{-\bullet}/Q_A$ FTIR difference spectrum using PS II core preparations form *Synechocystis* PCC 6803 where the imidazole nitrogens of histidine side chains are selectively labeled with ^{15}N. The double difference spectrum of the $Q_A^{-\bullet}/Q_A$ FTIR spectra between ^{15}N-labeled and unlabeled samples exhibits bands at 1474/1456/1444, 1359, 1256/1249, 1179/1169, 1109/1102/1090, 983/968, and 942 cm^{-1} (*37*). The bands at 1367/1336, 1251, 1183, and 1105/1093 in Figure 1c are in correspondence with the above mentioned frequencies of 1359, 1256/1249, 1179/1169, and 1109/1102/1090 cm^{-1} and are therefore most likely reflecting imidazole ring modes of a histidine side chain. As a consequence of this assignment, the state of histidine residue(s) coupled with Q_A is inferred to become somewhat altered when the non-heme iron center is extracted.

With respect to the nature of the histidines, the residues which coordinate the non-heme iron appear to be the most likely candidates. Among them, His 215 and 269 of polypeptide D2 are closest to $Q_A^{-\bullet}$. On the basis of recent Q-band EPR spectroscopy in Zn-substituted reaction centers from the purple bacterium *Rhodobacter sphaeroides* and the known crystal structure, the C_4⋯O oxygen was inferred to form a strong hydrogen bond with His 219 of the M-subunit (*38*). If one assumes an analogous structure for PS II and takes into account the similarities of the hydrogen bond pattern of $Q_A^{-\bullet}$ in purple bacteria and PS II (see ref *27* and references therein), it is expected that His 215 of polypeptide

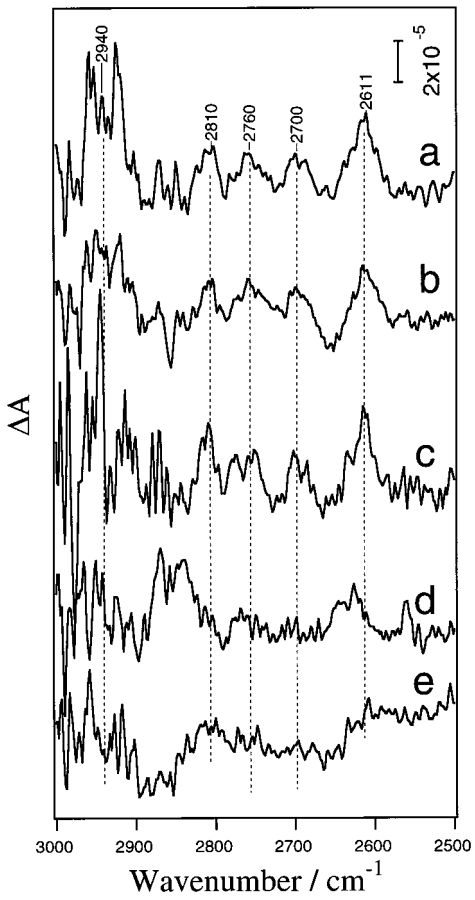

FIGURE 2: FTIR difference spectra of $Q_A^{-\bullet}/Q_A$ in the region of hydrogen-bonding NH stretching modes (2500−3000 cm^{-1}): (a) control sample at pH = 6.5; (b) non-heme iron-depleted sample at pH = 6.5; (c) control sample at pH = 8.0; (d) cyanide-treated sample at pH = 8.0; (e) high pH-treated (pH = 11) sample measured at pH = 11. For experimental details, see Materials and Methods.

D2, which is equivalent to the above mentioned His 219 of *Rh. sphaeroides*, exhibits the strongest interaction of the histidine residues with $Q_A^{-\bullet}$. Accordingly, the vibrations of His 215 (D2) are likely to be the most seriously affected upon $Q_A^{-\bullet}$ formation in PS II, thus giving rise to bands in the $Q_A^{-\bullet}/Q_A$ FTIR difference spectrum. Upon removal of the non-heme iron the vibrational modes of this histidine are somewhat changed, as reflected in the double difference spectrum shown in Figure 1c.

It is well known that a strongly hydrogen-bonding NH group of imidazole compounds exhibits a broad NH stretching band at around 2800 cm^{-1} with a number of subbands arising from Fermi resonance of overtones or combinations of fundamental vibrations (*39*). The $Q_A^{-\bullet}/Q_A$ difference spectra of the hydrogen-bonding NH stretching region (2500−3000 cm^{-1}) are shown in Figure 2. Spectrum a measured with control membranes at pH 6.5 exhibits peaks at 2611, 2700, 2760, 2810, and 2940 cm^{-1}. This assignment has been proven by [^{15}N]His labeling to be derived from the His modes (*37*). The appearance of these peaks in the $Q_A^{-\bullet}/Q_A$ difference spectrum indicates that (i) the His side chain is engaged in strong hydrogen bonding through the imidazole NH group, probably to the Q_A carbonyl, and (ii) the hydrogen-bonding structure is affected by $Q_A^{-\bullet}$ formation. The corresponding $Q_A^{-\bullet}/Q_A$ difference spectrum of the iron-depleted PS II preparation is depicted as spectrum b in Figure 2. A comparison with the untreated control (spectrum a) readily shows that the peaks on the hydrogen-bonding His NH are not changed when the non-heme iron is properly removed. This indicates that hydrogen bonding between Q_A and His (most likely His 215 of the D2 subunit) is hardly affected by iron removal.

The data reported so far provide clear evidence for the conclusion that both the C⋯O interaction of $Q_A^{-\bullet}$ and hydrogen bonding of the coupled His side chain remain virtually unaffected upon non-heme iron removal. On the other hand, vibrational modes of the imidazole ring of the His and the conformational change of the protein are affected by iron removal. However, these changes are not surprising because ring modes of His are expected to be modified when the metal coordination is lost and also the protein flexibility around the non-heme iron should increase after its removal. As a consequence, the response of these vibrations to $Q_A^{-\bullet}$ formation will be altered in the iron-depleted sample. The seemingly puzzling findings of virtually invariant bands in the NH stretching region together with ring modes which are changed upon iron removal might be rationalized by the possibility that the NH stretching mode is highly isolated from other ring vibrations (*40*) and thus less susceptible to the change in the imidazole ring. This interpretation, however, bears some problems because an isolated mode should not contribute to Fermi resonance and the latter bands are expected to undergo changes due to alterations of ring modes. Therefore, it appears attractive to consider the possibility that two different His residues (possibly His 215 and 269 of D2) contribute to the $Q_A^{-\bullet}/Q_A$ FTIR difference spectrum. This alternative would explain the incompatible behavior of ring vibrations and the band in the NH region.

With respect to the histidines, another problem will be briefly addressed, i.e., possible effects of protonation/deprotonation reactions. The p*K* value for the protonation of the imidazole moiety of histidines is about 6 in solution while that for the deprotonation is much higher (*41*). In proteins, however, significant changes can arise, especially by mutual interaction with other protonizable groups as shown by detailed calculations for bacterial reaction centers (*42*). An analogous effect could arise for the histidine ligands of the non-heme iron center and changes expected after its removal. Interestingly, the redox equilibrium between $Q_A^{-\bullet}Q_B$ and $Q_AQ_B^{-\bullet}$ was found to exhibit a marked pH dependence (*43*−*45*) with a p*K* value slightly higher than 7.6 (*44*). Accordingly, deprotonation of histidine residue(s) in the alkaline might be involved in this phenomenon. It is therefore attractive to analyze the FTIR difference spectra of control and iron-depleted PS II membrane fragments at higher pH. Check experiments of the flash-induced relative fluorescence quantum yield revealed that the formation of $Q_A^{-\bullet}$ and its stabilization by addition of DCMU and NH_2OH are virtually the same in the range from pH = 6.5 to pH 9 (Christen, Steffen, Kurreck, and Renger, unpublished results).

The FTIR difference spectra gathered at pH = 8.5 for both the control and iron-depleted samples and the double difference spectrum between them closely resemble those monitored at pH = 6.5 (data not shown). In particular, His bands in the NH stretching region (2500−3000 cm^{-1}) and the region of ring vibrations (1000−1400 cm^{-1}) remain

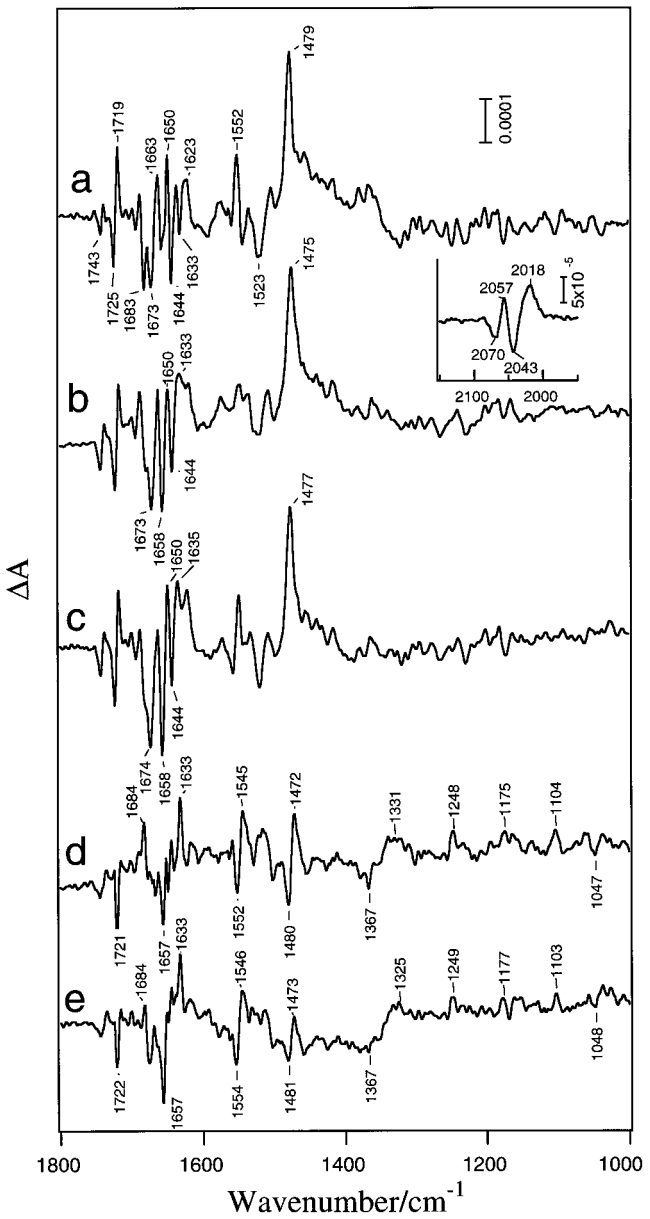

FIGURE 3: Light-induced FTIR difference spectra of PS II upon $Q_A^{-\bullet}$ formation measured in control PS II membranes at pH = 8.0 (trace a), cyanide-treated samples at pH = 8.0 (trace b), and high pH-treated (pH = 11) samples (trace c) measured at pH = 11. Traces d and e are the difference of spectra a and b (cyanide-treated minus control) and spectra a and c (high pH-treated minus control), respectively. For experimental details, see Materials and Methods. Inset: CN stretching region of the $Q_A^{-\bullet}/Q_A$ spectrum of the cyanide-treated sample at pH = 8.0.

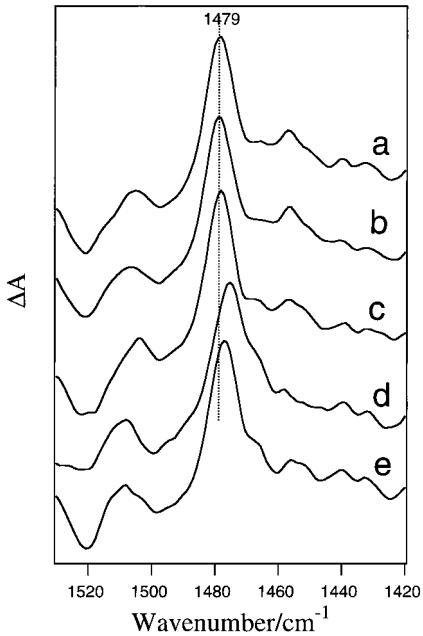

FIGURE 4: Comparison of the C⋯O stretching band of semiquinone in the $Q_A^{-\bullet}/Q_A$ FTIR difference spectra of various samples: (a) control sample at pH = 6.5; (b) iron-depleted sample at pH = 6.5; (c) control sample at pH = 8.0; (d) cyanide-treated sample at pH = 8.0; (e) high pH-treated (pH 11) sample measured at pH = 11.

virtually unaffected. These findings indicate that no change of the protonation state of the histidine(s) coupled to Q_A takes place when the pH is shifted from 6.5 to 8.5, and thus this His residue is not directly related to the pH dependence of the redox equilibrium between $Q_A^{-\bullet}Q_B$ and $Q_AQ_B^{-\bullet}$.

Cyanide-Treated and High pH-Treated PS II Membranes. Figure 3 compiles the $Q_A^{-\bullet}/Q_A$ difference spectra of Tris-washed PS II membranes (spectrum a) and those of samples that were subsequently treated either with cyanide at pH 8.0 (spectrum b) or with high pH (pH 11) (spectrum c). The control spectrum (Figure 3a) at pH 8.0 is virtually identical to the spectrum at pH 6.5 (Figure 1a), indicating that the difference of Tris washing and NH_2OH treatment to remove the Mn cluster (the 33 kDa extrinsic protein is present in the NH_2OH-treated preparation but not in the Tris-treated one) does not affect the $Q_A^{-\bullet}/Q_A$ spectrum. A comparison of spectra b and c with spectrum a readily reveals that noticable changes arise in the C⋯O stretching band of $Q_A^{-\bullet}$ upon cyanide and high pH treatment: the band at 1479 cm^{-1} in the control sample undergoes downshifts to 1475 and 1477 cm^{-1} in the cyanide-treated and high pH-treated samples, respectively. These shifts are more clearly illustrated in the expanded spectra in Figure 4. It shows that the C⋯O band position remains the same in the control at pH 6.5 (a) and pH 8.0 (c) and in the iron-depleted samples (b). In marked contrast, a significant shift by 4 and 2 cm^{-1} to lower frequencies is observed in cyanide-treated (d) and high pH-treated (e) samples, respectively. This observation indicates that the mode of the hydrogen bonding of C⋯O in $Q_A^{-\bullet}$ is altered by both the cyanide and high pH treatments, more drastically by the former than the latter treatment. Other prominent changes in the $Q_A^{-\bullet}/Q_A$ spectrum upon cyanide and high pH treatments were observed in the amide I region (1600−1700 cm^{-1}). Spectral changes were similar in both spectra of cyanide-treated and high pH-treated samples (Figure 3b,c): the band at 1683 cm^{-1} in the control spectrum (Figure 3a) disappeared, and the intensity of the negative band at 1658 cm^{-1} and the positive band at 1633−1635 cm^{-1} increased.

Double difference spectra of $Q_A^{-\bullet}/Q_A$ between the control (pH 8.0) and CN^--treated samples and between the control (pH 8.0) and high pH-treated samples are presented in panels d and e of Figure 3, respectively. The band pattern was very similar between the two spectra. In particular, several bands at 1100−1400 cm^{-1}, which are most likely assigned to the modes of the His side chain (*37*), the 1633/1657 cm^{-1} bands in the amide I region, and 1545−6/1552−4 cm^{-1} bands in the amide II region are basically identical. Differential signals

at 1472/1480 cm^{-1} (Figure 3d) and at 1473/1481 cm^{-1} (Figure 3e) reflect shifts of the 1479 cm^{-1} band of the C⋯O vibration of $Q_A^{-\bullet}$. In marked contrast, such a shift is not observed for the iron-depleted sample (see Figure 1c). On the other hand, the spectral features of the double difference spectra for all three sample types (iron depleted, CN treated, and high pH) are very similar (compare Figure 1c with Figure 3d,e) in the amide I region and the region of imidazole ring vibrations. The latter observation indicates that all three treatments give rise to similar structural effects on the conformations of the surrounding protein and the imidazole ring coupled to Q_A whereas the effect on the hydrogen bonding of Q_A is quite different (vide supra). In order to explain these phenomena, one could assume that the CN^- and high pH treatments lead to a break of the coordination of His 215 (D2) to the non-heme iron by ligation with CN^- and OH^- anions, thus causing perturbations of His and its microenvironment similar to those caused by Fe depletion, except that the hydrogen bonding to Q_A remains unaffected in the latter sample (vide infra). Coordination of the CN^- anion was in fact revealed in the CN stretching region of the $Q_A^{-\bullet}/Q_A$ spectrum of the CN^--treated sample (Figure 3b, inset). Two differential signals at 2070/2057 and 2043/2018 cm^{-1} were clearly observed. This result suggests that at least two CN^- ions are attached to the non-heme iron or present in the vicinity of Q_A in the CN^--treated PS II.

The NH stretching regions of the $Q_A^{-\bullet}/Q_A$ difference spectra of the control (pH 8.0), cyanide-treated, and high pH-treated samples are presented in panels c, d, and e of Figure 2, respectively. In the control spectrum at pH 8.0, several peaks in this region were basically identical to those of the control sample at pH 6.5 (Figure 2a) and the non-heme iron-depleted sample (Figure 2b). In contrast, upon cyanide and high pH treatments, these peaks were clearly lost, indicating that the hydrogen-bonding interaction of the His side chain is drastically changed. The most plausible explanation for this phenomenon is the assumption that hydrogen bonding between Q_A and imidazole has been broken due to these treatments and thus the NH vibrations of His do not respond to the $Q_A^{-\bullet}$ formation. The appearance of His bands in the double difference spectra (Figure 3d,e) might also be explained by a loss of the His bands upon cyanide and high pH treatments. It is noted that in the spectra of the cyanide-treated sample (Figure 2d) a few bands remain in different positions compared with the His peaks of the control spectra. Although the origin of these bands is not known, it is unlikely that they arise from a different form of the His side chain that is generated by CN^- treatment. Because the peak positions are attributed to harmonics or combinations of the fundamental modes (*39*), drastic changes of the His vibrations are necessary to explain the large frequency shifts. If the fundamental vibrations would largely be changed while the His still remains coupled to Q_A, then these modes will appear in the double difference spectrum in the lower frequency region (1000−1600 cm^{-1}). However, the band pattern of the His modes observed in the double difference spectra between control and cyanide-treated sample (Figure 3d) was almost identical to that of the iron-depleted sample (Figure 1c). The loss of strong hydrogen bonding between the Q_A carbonyl and histidine NH groups in the cyanide-treated and high pH-treated samples is consistent with the shift of the C⋯O band of $Q_A^{-\bullet}$ (Figure 4). The smaller shift observed in the high pH-treated PS II membrane fragments might be due to the formation of new hydrogen bonding between a hydroxyl anion and $Q_A^{-\bullet}$. The shift of the C⋯O band to lower frequencies caused by the breakage of a hydrogen bond seems to be peculiar. However, since this band is a coupled mode of two C⋯O and two C═C vibrations, a change in the symmetry of the molecular interactions may significantly affect the direction of the shift. Further experimental and theoretical studies of this effect of symmetry are necessary in order to draw an unequivocal conclusion about the change in the C⋯O interaction. Previous ESEEM studies showed that magnetic coupling of $Q_A^{-\bullet}$ with an imidazole nitrogen was present in iron-depleted (*28*) and high pH-treated PS II (*20*), whereas in CN^--treated PS II the coupling was absent (*19*, *28*, *46*, *47*) or significantly altered (*22*). The present FTIR results indicating that the hydrogen bonding of $Q_A^{-\bullet}$ with a His NH group is unaffected upon Fe depletion but ruptured upon CN^- treatment are basically consistent with the ESEEM results. On the other hand, in the high pH-treated sample, the FTIR result of the absence of hydrogen bonding is in disagreement with the conclusion from the ESEEM study. This inconsistency may be explained by deprotonation of the His imidazole at high pH (pH 11); i.e., although hydrogen bonding between $Q_A^{-\bullet}$ and His is lost by this deprotonation, the imidazole nitrogen may stay at the same position and thus the magnetic coupling with $Q_A^{-\bullet}$ could still remain.

CONCLUDING REMARKS

The present study reveals that, after suitable depletion of the non-heme iron from PS II membrane fragments (*24*), the hydrogen-bonding interaction of $Q_A^{-\bullet}$ is virtually unaffected, especially the hydrogen bond with a His side chain (most likely His 215 of the D2 subunit). In marked contrast, upon cyanide and high pH treatments, the hydrogen bonding between $Q_A^{-\bullet}$ and His seems to be lost. Although all three treatments show some alteration in the protein conformation and imidazole ring modes, it is suggested that the immediate molecular interaction of $Q_A^{-\bullet}$ is rather intact in the iron-depleted sample. This conclusion gains support by the finding that the kinetics of electron transfer from $Pheo^{-\bullet}$ to Q_A (*28*, *48*) remains almost unaffected (within a span of 25%) after removal of the non-heme iron center. As a consequence, it is inferred that the information gathered from EPR, ^1H-ENDOR (*27*), and ESEEM studies (*28*) on the interaction of $Q_A^{-\bullet}$ with the protein environment in iron-depleted samples mainly reflects the normal situation in the presence of the non-heme iron center.

REFERENCES

1. Renger, G. (1997) *Physiol. Plant 100*, 828−841.
2. Crofts, A. R., and Wraight, C. A. (1983) *Biochim. Biophys. Acta 726*, 149−185.
3. Lavergne, J., and Briantais, J.-M. (1996) in *Advances in Photosynthesis* (Yocum, C. A., and Ort, D. R., Eds.) Vol. 4, pp 265−287, Kluwer Academic Press, Dordrecht.
4. Trebst, A. (1986) *Z. Naturforsch. 41c*, 240−245.
5. Michel, H., and Deisenhofer, J. (1988) *Biochemistry 27*, 1−7.
6. Stowell, M. H. B., McPhillips, T. M., Rees, D. C., Soltis, S. M., Abresch, E., and Feher, G. (1997) *Science 276*, 812−816.

7. Reifarth, F., and Renger, G. (1998) *FEBS Lett. 428*, 123−126.
8. Garbers, A., Reifarth, F., Kurreck, J., Renger, G., and Parak, F. (1998) *Biochemistry 37*, 11399−11404.
9. Deisenhofer, J., and Michel, H. (1989) *EMBO J. 8*, 2149−2170.
10. Feher, G., Allen, J. P., Okamura, M. Y., and Lubitz, W. (1989) *Nature 339*, 111−116.
11. Hienerwadel, R., and Berthomieu, C. (1995) *Biochemistry 34*, 16288−16297.
12. Bowes, J. M., Crofts, C. A., and Itoh, S. (1979) *Biochim. Biophys. Acta 547*, 320−335.
13. Petrouleas, V., and Diner, B. A. (1986) *FEBS Lett. 147*, 111−114.
14. Renger, G., Wacker, U., and Völker, M. (1987) *Photosynth. Res. 13*, 167−184.
15. Diner, B. A., and Petrouleas, V. (1987) *Biochim. Biophys. Acta 895*, 107−125.
16. Parak, F., Frolov, E. N., Kononenko, A. A., Mössbauer, R. L., Goldanskii, V. I., and Rubin, A. B. (1980) *FEBS Lett.*, 368−372.
17. Garbers, A., Kurreck, J., Reifarth, F., Renger, G., and Parak, F. (1996) *Proc. Int. Conf. Appl. Mössbauer Effect* (Ortalli, I., Ed.) Vol. 50, pp 811−814, SIF, Bologna.
18. Sanakis, Y., Petrouleas, V., and Diner, B. A. (1994) *Biochemistry 33*, 9922−9928.
19. Deligiannakis, Y., Boussac, A., and Rutherford, A. W. (1995) *Biochemistry 34*, 16030−16038.
20. Deligiannakis, Y., Jegerschöld, C., and Rutherford, A. W. (1997) *Chem. Phys. Lett. 270*, 564−572.
21. Klimov, V. V., Dolan, E., Shaw, E. R., and Ke, B. (1980) *Proc. Natl. Acad. Sci. U.S.A. 77*, 7227−7231.
22. Astashkin, A. V., Hara, H., Kuroiwa, S., Kawamori, A., and Akabori, K. (1998) *J. Chem. Phys. 108*, 10143−10151.
23. MacMillan, F., Gleiter, H., Renger, G., and Lubitz, W. (1990) in *Current Research in Photosynthesis* (Baltscheffsky, M., Ed.) Vol. 1, pp 531−534, Kluwer, Dordrecht.
24. Kurreck, J., Garbers, A., Reifarth, F., Andréasson, L.-E., Parak, F., and Renger, G. (1996) *FEBS Lett. 381*, 53−57.
25. Zech, S. G., Kurreck, J., Eckert, H.-J., Renger, G., Lubitz, W., and Bittl, R. (1997) *FEBS Lett. 414*, 454−456.
26. Zech, S. G., Kurreck, J., Renger, G., Lubitz, W., and Bittl, R. (1999) *FEBS Lett. 442*, 79−82.
27. MacMillan, F., Lendzian, F., Renger, G., and Lubitz, W. (1995) *Biochemistry 34*, 8144−8156.
28. Renger, G., Kurreck, J., Haag, E., Reifarth, F., Bergmann, A., Parak, F., Garbers, A., McMillan, F., Lendzian, F., and Lubitz, W. (1997) in *Bioinorganic Chemistry* (Trautwein, A., Ed.) pp 260−277, Wiley−VCH Publishers, Weinheim.
29. Berthold, D. A., Babcock, G. T., and Yocum, C. F. (1981) *FEBS Lett. 134*, 231−234.
30. Völker, M., Ono, T., Inoue, Y., and Renger, G. (1985) *Biochim. Biophys. Acta 806*, 25−34.
31. Noguchi, T., Mitsuka, T., and Inoue, Y. (1994) *FEBS Lett. 356*, 179−182.
32. Noguchi, T., Ono, T., and Inoue, Y. (1995) *Biochim. Biophys. Acta 1232*, 59−66.
33. Berthomieu, C., Nabedryk, E., Mäntele, W., and Breton, J. (1990) *FEBS Lett. 269*, 363−367.
34. Hienerwadel, R., Boussac, A., Breton, J., and Berthomieu, C. (1996) *Biochemistry 35*, 15447−25460.
35. Xiong, J., Subramaniam, S., and Govindjee (1996) *Protein Sci. 5*, 2054−2073.
36. Svensson, B., Etchebest, C., Tuffery, P., van Kan, P., Smith, J., and Styring, S. (1996) *Biochemistry 35*, 14486−14503.
37. Noguchi, T., Inoue, Y., and Tang, X.-S. (1999) *Biochemistry 38*, 399−403.
38. Isaacson, R. A., Abresch, E. C., Lendzian, F., Boullais, C., Paddock, M. L., Mioskowski, C., Lubitz, W., and Feher, G. (1996) in *The Reaction Centre of Photosynthetic Bacteria—Structure and Dynamics* (Michel-Beyerle, M.-E., Ed.) pp 353−367, Springer, Berlin.
39. Wolff, H., and Wolff, E. (1971) *Spectrochim. Acta 27A*, 2109−2118.
40. Majouba, M., Millié, Ph., and Vergotan, G. (1995) *J. Mol. Struct. 344*, 21−36.
41. Timasheff, S. N. (1962) in *Biological Macromolecules. Biological Polyelectrolytes* (Veis, A., Ed.) Vol. III, pp 1−66, Marcel Dekker Inc., New York.
42. Beroza, P., Fredkin, D. R., Okamura, M., and Feher, G. (1995) *Biophys. J. 69*, 2233−2250.
43. Rutherford, A. W., Renger, G., Koike, H., and Inoue, Y. (1984) *Biochim. Biophys. Acta 767*, 548−556.
44. Robinson, H. H., and Crofts, A. R. (1984) in *Advances in Photosynthesis Research* (Sybesma, C., Ed.) Vol. 1, pp 477−480, M. Nijhoff/Dr. W. Junk Publishers, The Hague.
45. Vermaas, W. F. J., Renger, G., and Dohnt, G. (1984) *Biochim. Biophys. Acta 764*, 194−202.
46. Tang, X.-S., Peloquin, J. M., Lorigan, G. A., Britt, R. D., and Diner, B. A. (1995) in *Photosynthesis: from Light to Biosphere* (Mathis, P., Ed.) Vol. 1, pp 775−778, Kluwer Academic Publishers, Dordrecht.
47. MacMillan, F., Kurreck, J., Adir, N., Lendzian, F., Käss, H., Reifarth, F., Renger, G., and Lubitz, W. (1995) in *Photosynthesis: from Light to Biosphere* (Mathis, P., Ed.) Vol. 1 pp 659−662, Kluwer Academic Publishers, Dordrecht.
48. Bernarding, J., Eckert, H.-J., Eichler, H. J., Napiwotzki, A., and Renger, G. (1994) *Photochem. Photobiol. 59*, 566−573.

BI981759E